Scripta Materialia 136 (2017) 136–140

Contents lists available at ScienceDirect

Scripta Materialia

journal homepage: www.elsevier.com/locate/scriptamat

Regular Article

Gamma-gamma prime-gamma double prime dual-superlattice superalloys

P.M. Mignanelli [a], N.G. Jones [a], E.J. Pickering [a,b], O.M.D.M. Messé [a], C.M.F. Rae [a], M.C. Hardy [c], H.J. Stone [a,*]

[a] Department of Materials Science and Metallurgy, University of Cambridge, Cambridge CB3 0FS, UK
[b] The School of Materials, The University of Manchester, Manchester M13 9PL, UK
[c] Rolls-Royce plc, PO BOX 31, Derby DE24 8BJ, UK

ARTICLE INFO

Article history:
Received 23 February 2017
Received in revised form 18 April 2017
Accepted 18 April 2017
Available online 3 May 2017

Keywords:
Nickel alloys
Superalloy
Transmission electron microscopy

ABSTRACT

Improving the efficiency of gas turbine engines requires the development of new materials capable of operating at higher temperatures and stresses. Here, we report on a new polycrystalline nickel-base superalloy that has exceptional strength and thermal stability. These properties have been achieved through a four-element composition that can form both gamma prime and gamma double prime precipitates in comparable volume fractions, creating an unusual dual-superlattice microstructure. Alloying studies have shown that further property improvements can be achieved, and that with development such alloys may be suitable for future engine applications.

The global drive to reduce emissions and improve efficiency in the civil aviation and power generation industries demands the development of new gas turbine engines with higher gas stream temperatures and faster rotational speeds [1]. These service conditions cannot be tolerated by existing Ni-base superalloys and new alloys are therefore required. Ni-base superalloys derive many of their excellent mechanical properties from dispersions of fine-scale precipitates that have superlattice structures of the face-centred cubic gamma (γ) matrix in which they reside [2–3]. These precipitates impede the motion of dislocations through the material due to the energy penalty associated with the faulting of the precipitates following the passage of a single dislocation and are used during thermo-mechanical processing to control the grain size. The Ni-base superalloys currently used at the highest service temperatures are strengthened by cubic Ni_3Al gamma prime (γ') precipitates. In contrast, the most widely used superalloy, Inconel 718 (IN718, Ni-20.5Cr-18.85Fe-0.33Co-1.84Mo-1.18Al-3.3Nb-1.23Ti-0.34C-0.02B at.% [4]), is reinforced by tetragonal Ni_3Nb gamma double prime (γ'') precipitates. The additional strengthening conveyed by γ'' over γ' is a function of the coherency of the precipitates with the matrix and the distortion caused by the *c*-axis of the tetragonal γ'' [5]. However, such alloys are limited to lower-temperature applications, as above 650 °C the γ'' phase decomposes to the thermodynamically stable δ phase, with a concomitant deterioration in strength [6–7].

Efforts to improve the temperature capability of IN718 have adopted two differing approaches. Firstly, compositional changes and controlled heat treatments have been used to modify the morphology of the precipitates [8]. These changes resulted in a "compact-morphology" precipitate, consisting of a cube-shaped γ' core with a shell of γ'' coating the surface, producing a thermal stability greater than that of conventional IN718. Secondly, more dramatic compositional modifications to IN718 have been explored [9]. Through increasing both the Al + Ti content and raising the Al/Ti ratio it was shown that the coarsening kinetics of the γ'' was retarded and that the precipitation of the δ phase was delayed, resulting in an increased thermal stability to IN718 type alloys.

In a recent systematic study of Ni-Cr-Al-Nb alloys, only γ and γ' phases were observed to form in compositions with Al:Nb ratios between 2.3 and 1 [10]. Conversely, commercial alloys with low Al:Nb ratios, <0.3, are known to preferentially form the γ'' phase [7]. These results suggest that intermediate compositions should allow both types of precipitate to co-exist. Indeed, some commercial alloys do have Al:Nb ratios in this range and contain γ' and γ'' phases. However, such alloys have compositions biased towards either end of the range, leading to microstructures dominated by one precipitate phase. For example, IN718 contains ~3% γ' and ~20% γ''. Through experimental exploration of the intermediate composition space, we have identified superalloy compositions [11] with microstructures containing comparable fractions of both γ' and γ'' precipitates, which exhibit excellent strength and microstructural stability.

Ingots of Ni-15Cr-4Al-6Nb (at.%) were produced by vacuum induction or vacuum arc melting from elemental metals with purity ≥99.9%. To assess the effect of alloying on the microstructure and properties, additional ingots were prepared using the same route with direct at.% substitutions of Ni by 1 or 2% Mo, 1 or 2% W, 2 or 6% Cr, 4 or 8% Fe, 4, 8 or 12% Co. A larger quantity of Ni-17Cr-4Al-6Nb-0.15C-0.16B-0.0375Zr (at.%) for mechanical testing was also produced by ATI Powder Metals through a commercial powder metallurgy route, including hot isostatic pressing,

* Corresponding author.
E-mail addresses: pmm46@cam.ac.uk (P.M. Mignanelli), ngj22@cam.ac.uk (N.G. Jones), ed.pickering@manchester.ac.uk (E.J. Pickering), omdmm2@cam.ac.uk (O.M.D.M. Messé), cr18@cam.ac.uk (C.M.F. Rae), mark.hardy@rolls-royce.com (M.C. Hardy), hjs1002@cam.ac.uk (H.J. Stone).

http://dx.doi.org/10.1016/j.scriptamat.2017.04.029

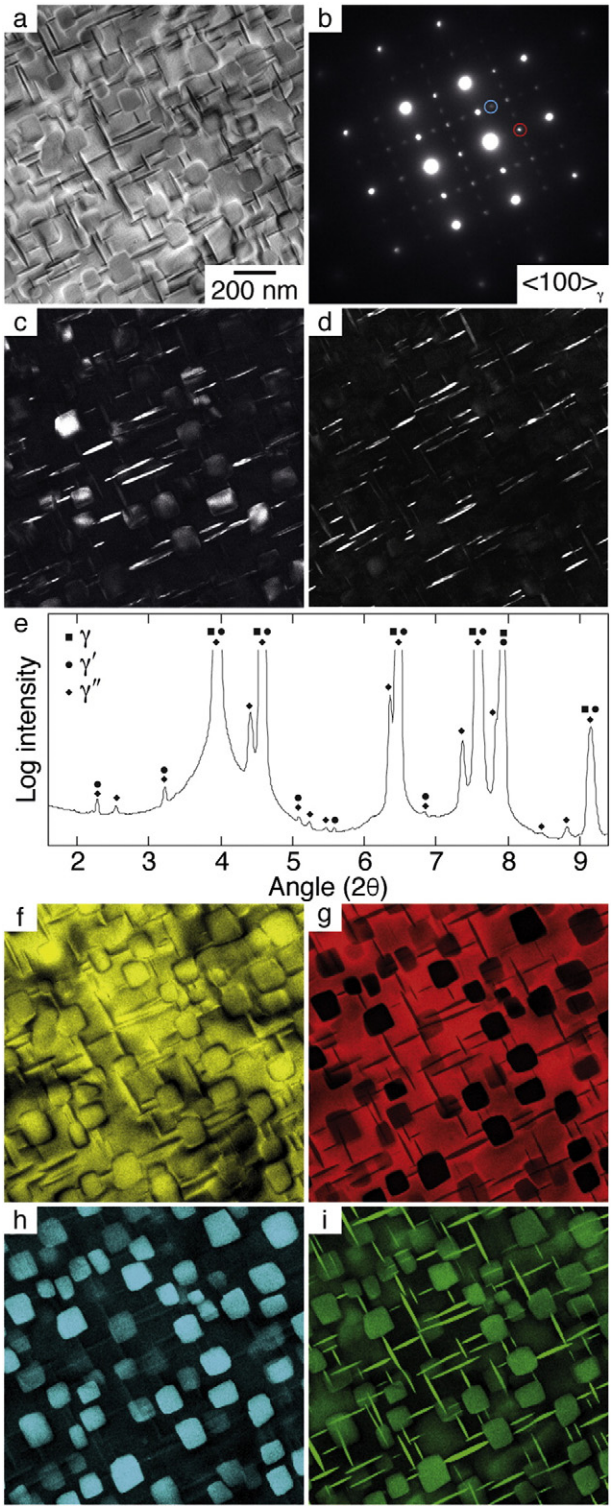

Fig. 1. The dual-superlattice microstructure after heat treatment at 1200 °C for 4 h followed by 700 °C for 1000 h. (a) STEM bright field image and (b) corresponding electron diffraction pattern along 〈001〉 $_{\gamma}$, (c) dark field image acquired using the superlattice reflection encircled in red showing both cuboidal and acicular precipitates and (d) dark field image acquired using the superlattice reflections encircled in blue showing only acicular precipitates, (e) high energy synchrotron X-ray diffraction spectrum, containing characteristic peaks from the γ, γ′ and γ″ phases, STEM EDX elemental distribution maps of (f) Ni, (g), Cr (h) Al and (i) Nb.

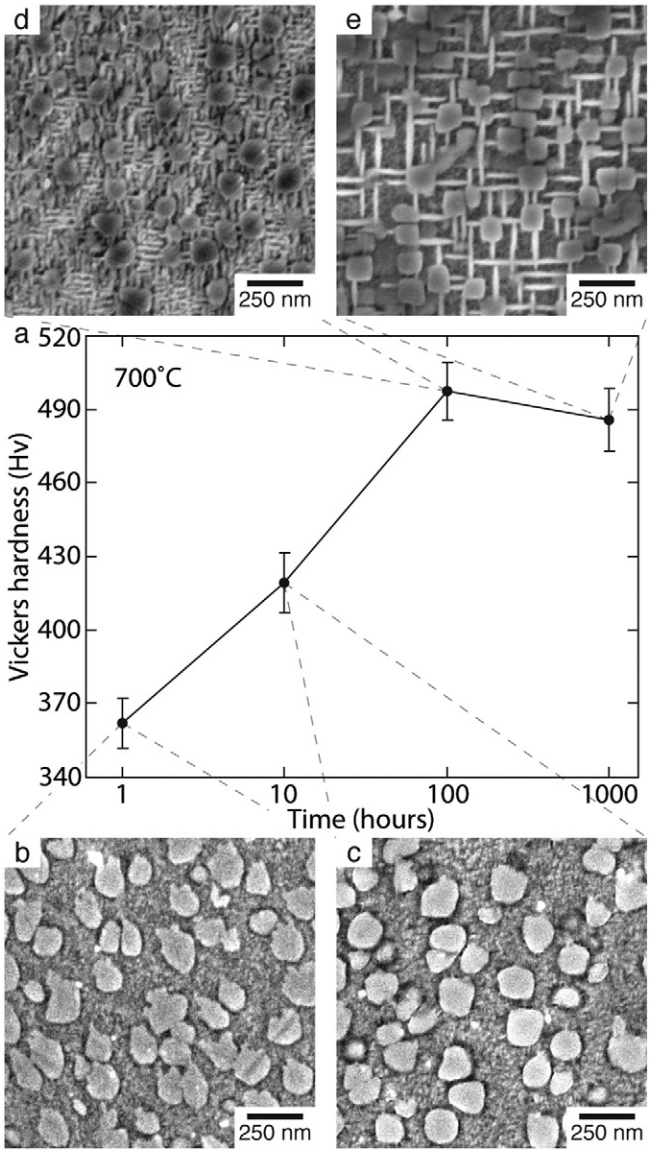

Fig. 2. The effect of heat treatment time at 700 °C (following solution treatment) on the room temperature Vickers hardness and the microstructure of the base composition alloy Ni-15Cr-4Al-6Nb (at.%). (a) The variation in room temperature hardness, (b) the microstructure after 1 h at 700 °C, (c) the microstructure after 10 h at 700 °C, (d) the microstructure after 100 h at 700 °C and (e) the microstructure after 1000 h at 700 °C. Errors were calculated as the standard deviation of 10 individual measurements of the alloy hardness.

isothermal forging and heat treatment. All alloys were solution heat treated for 4 h at 1200 °C in evacuated and argon backfilled glass ampoules. Thermal exposures of the alloys were performed at temperatures between 600 and 900 °C for durations of 1, 10, 100, 500 and 1000 h. Hardness data were obtained using a Vickers indenter with a 30 kg mass and 30 s dwell and errors calculated as the standard deviation of 10 individual measurements. Synchrotron X-ray diffraction data were collected on the I12 beamline at the Diamond Light Source, Didcot, UK under experiment EE9270. Scanning electron-imaging microscopy was completed using a FEI Nova NanoSEM 450 and transmission electron microscopy (TEM) was performed using an FEI Tecnai Osiris. Dislocation imaging was conducted in high-angle annular dark field (HAADF) scanning transmission electron microscopy (STEM) mode as the high level of strain in the sample prevented the use of conventional TEM modes. Ambient and elevated temperature tensile testing was performed under BS EN ISO 6892-2: 2009 at Swansea Materials Research & Testing Ltd., Swansea, UK.

The microstructure of the alloy with composition Ni-15Cr-4Al-6Nb (at.%) after solution treatment and ageing at 700 °C for 1000 h is shown in Fig. 1a and contains appreciable and comparable volume

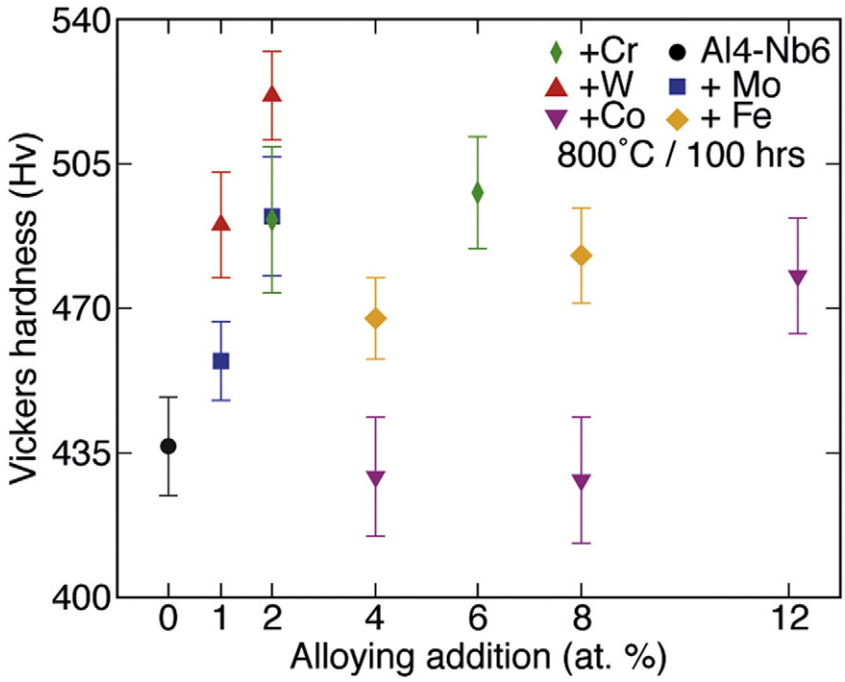

Fig. 3. The effect of alloying on the room temperature hardness of the dual-superlattice superalloy with base composition Ni-15Cr-4Al-6Nb (at.%) solution treated and aged at 800 °C for 100 h. Errors were calculated as the standard deviation of 10 individual measurements of the alloy hardness.

fractions of the two precipitates, ~25% γ′ and ~20% γ″. An electron diffraction pattern acquired along $[001]_{\gamma}$, Fig. 1b, contained reflections from both superlattice structures, in addition to those from the γ matrix. Dark field electron imaging, using different superlattice reflections enabled the cuboidal precipitates to be identified as the γ′ phase and the acicular precipitates as the γ″ phase, as shown in Fig. 1c–d. Further evidence of their co-existence was established through high-energy synchrotron X-ray diffraction, Fig. 1e, which showed characteristic peaks from their respective structures. The elemental partitioning between the phases was elucidated through compositional mapping using TEM based energy-dispersive X-ray spectroscopy, Fig. 1f–i. The cuboidal precipitates were found to be rich in Ni and Al, whilst also containing Nb, consistent with a Ni_3Al based γ′ phase. In contrast, the acicular precipitates were found to be rich in Ni and Nb, indicative of the Ni_3Nb γ″ phase, which is known to possess limited solubility for Al [12].

The evolution of the alloy's microstructure and hardness as a function of heat treatment time at 700 °C, post solution treatment, is shown in Fig. 2. Following cooling from the solution treatment, only γ′ precipitates were observed and the alloy's hardness in this state was approximately 300 Hv. Subsequent heat treatment at 700 °C, which is below the γ″ solvus of ~927 °C determined by synchrotron X-ray diffraction, enabled the γ″ phase to form. Analysis of the γ′ phase in the microstructure revealed a decrease in the volume fraction from 30 to 25% between 1 and 10 h, but for longer duration exposures the amount of the γ′ phase remained approximately constant. Over the course of 100 h at 700 °C, Fig. 2b–d, a regular network of acicular γ″ precipitates was established and coarsened, leading to a peak hardness of ~500 Hv. During ageing at higher temperatures the peak strengths were achieved following shorter exposures, ~10 h at both 750 and 800 °C. The age hardening behaviour of the alloy offers potential benefits over many other superalloys in terms of the processing, forming and machining operations required to manufacture a component. The inability to suppress γ′ formation in Ni-base superalloys through rapid cooling results in intrinsically hard materials. Therefore, superalloys that contain large volume fractions of γ′, such as those used in higher temperature applications, are difficult to process and require forming at temperatures close to their γ′ solvus. Conversely, superalloys that are more amenable to forming operations inevitably include reduced γ′ volume fractions and therefore lower high temperature strength. Notably, the superalloy composition reported here contains only low γ′ volume fractions, potentially allowing it to be processed in the softer solution treated state, but may be subsequently strengthened by γ″ formation during the precipitation treatment. This offers the prospect of lower processing costs than conventional high temperature superalloys as well as the potential to fabricate components with more complex geometries.

In service, Ni-base superalloys are required to operate for prolonged periods at elevated temperatures without undergoing considerable microstructural evolution, which may result in property degradation and necessitate component retirement. Critically, the γ-γ′-γ″ microstructure remained stable after 1000 hour exposure at 700 °C, Fig. 2e. Following 1000 h at 700 °C, coarsening of the γ″ phase and a reduction in the volume fraction was observed. Encouragingly, this was associated with only a limited reduction in the alloy's hardness and no evidence of δ phase precipitation. The undesirable δ phase was observed to form following exposure at higher temperatures, after 500 h at 800 °C and between 10 and 100 h at 900 °C. The occurrence of this phase demonstrates that the γ″ phase is metastable and that δ phase formation must be expected after extended periods at elevated temperatures, which is consistent with unconstrained thermodynamic predictions for this alloy. However, as the γ-γ′-γ″ microstructure was retained with no evidence of the δ phase after 1000 h at 700 °C, this class of alloys offer considerably superior stability than IN718, in which the δ phase forms within 100 h at 700 °C and 1 h at 800 °C [13]. The increased stability of the dual-superlattice microstructure is thought to be a result of the presence of the appreciable volume fraction of γ′ precipitates that kinetically inhibit the transformation of γ″ to δ. This is consistent with previous studies of IN718, which have indicated that a higher γ′ volume fraction reduces the coarsening rate of the γ″ precipitates, and suppresses the formation of δ [9,14].

Ni-base superalloys commonly employ high concentrations of additional alloying elements in order to enhance their mechanical properties and resistance to environmental degradation [15–17]. To assess the extent to which the properties of the dual-superlattice superalloy investigated here may be improved through solid solution strengthening, the effect of Co, Cr, Fe, Mo and W were studied on material solution treated

and aged at 800 °C for 100 h. It was observed that the increase in exposure temperature of 100 °C produced a debit of ~60 Hv to the base material presented in Fig. 2 and, with the exception of Co, all of the elemental additions increased the hardness of the alloy, as shown in Fig. 3. Whilst additions of W provided the greatest degree of hardening, surpassing the peak hardness of the base alloy achieved with heat treatment at 700 °C, presented in Fig. 2, they led to a loss of morphological distinction between the γ′ and γ″ phases in the dual-superlattice microstructure that may compromise other properties. In contrast, alloying with Cr and Mo did not alter the microstructure and provided a significant degree of strengthening; offsetting the hardness debit due to the 100 °C temperature increase. These results suggest that further improvements could be achieved with judicious additions. Similarly, alloying with Fe did not modify the microstructure, although it only provided limited additional strength to the material. However, this may be useful as a potential route to reduce alloy cost.

Alongside the mechanical properties required of materials for use within gas turbine engines, excellent environmental resistance is necessary in order to withstand the high temperatures and corrosive atmosphere. Studies on the fatigue behaviour of IN718 have considered the formation of brittle niobium oxide films to be critical in determining the crack growth rates, in particular, the oxidation of NbC particles found at the grain boundaries [18]. As such, oxidation testing of the base alloy (Ni-15Cr-4Al-6Nb (at.%)) was conducted at 700 °C. Short-term oxidation exposures revealed mass gain rates similar to that of IN718 up to 100 h following transient oxidation. The results of a 1000 h isothermal exposure in air revealed that the maximum depth of damage was ~1.5 μm, consisting of a ~0.3 μm oxide scale with ~1.2 μm alumina fingers penetrating into the bulk. The use of laboratory X-ray diffraction equipment allowed the identification of the oxide scale species, which were found to be Cr_2O_3 and a $NbCrO_4$ spinel, with Al_2O_3 detected in very small amounts. The presence of δ phase was also detected in the laboratory X-ray diffraction of the surface, which was not detected in the sample bulk.

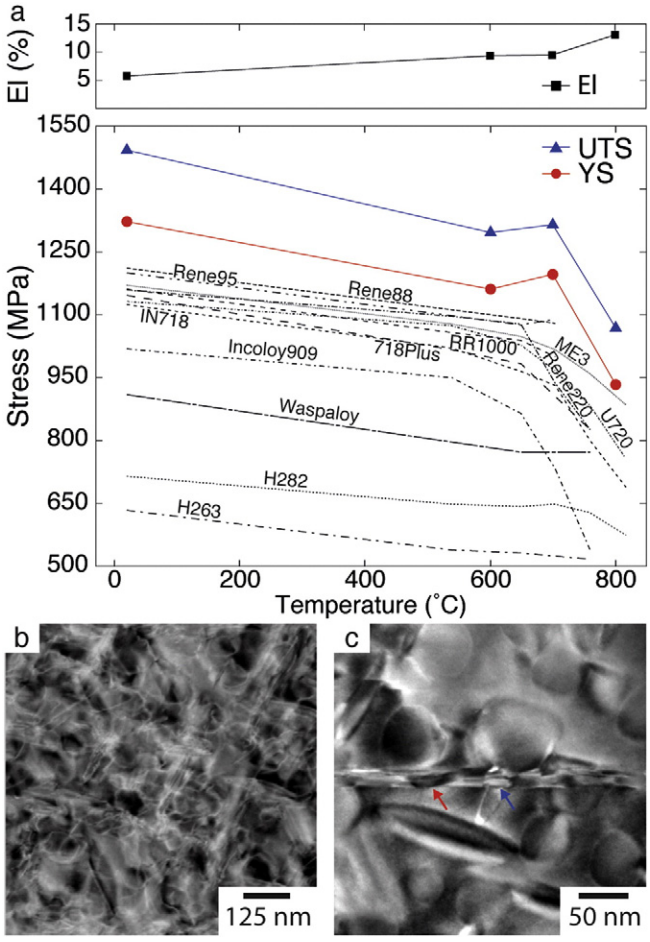

Fig. 4. The variation in yield strength (YS), ultimate tensile strength (UTS) and elongation to failure (El) as a function of temperature, alongside dislocation network imaging, of the dual-superlattice superalloy. (a) Comparison of the YS and UTS as a function of temperature with the yield strengths of 718Plus [19], Haynes 263 [20], Haynes 282 [21], IN718 [22], Incoloy 909 [23], ME3 [24], Rene 88 [25], Rene 95 [26], RR1000 [27], U720 [28], Rene 220 [29] and Waspaloy [20]. (b) and (c) HAADF STEM images of the sample tested at 700 °C imaged down the [110] zone axis showing the dislocation networks. (b) shows evidence of distinct shear bands and cross slip between {111} planes and (c) shows a magnified view of the shearing of the γ′ and γ″ precipitates.

To assess the tensile properties of γ-γ′-γ″ dual-superlattice superalloys, an alloy with composition Ni-17Cr-4Al-6Nb-0.15C-0.16B-0.0375Zr (at.%) was produced and processed through a standard powder metallurgy route. Minor elemental additions were included in the alloy to provide improved grain boundary strength, in line with established industry practice for polycrystalline Ni-base superalloys [11,15–17]. Ambient and elevated temperature tensile testing of this alloy showed that it possessed exceptional strength, Fig. 4a. For comparison, the yield strengths of a number of widely used, commercially available polycrystalline Ni-base superalloys are plotted as a function of temperature in this figure. At room temperature, the yield strength of the new dual-superlattice superalloy was >100 MPa higher than all of the commercial superalloy comparators. This superior strength was maintained across all of the temperatures considered, albeit to a lesser extent at temperatures in excess of 750 °C. Critically, these strengths were also achieved whilst retaining reasonable levels of tensile ductility, in the range 6–13%. This strength benefit was directly attributed to the dual-superlattice microstructure, as the alloy contained lower concentrations of solid solution strengthening elements than many of the other alloys shown in Fig. 4 and, with a grain size of ~65 μm, would not be expected to exhibit Hall-Petch strengthening above that of the commercial alloys, which typically have grain sizes <30 μm [24–28]. It is known that the strengthening benefit of the γ″ outweighs that of γ′ on a normalised volume fraction basis. However, the precipitation of the γ″ phase is limited to volume fractions of approximately 20% [30] due to the effect of impinging strain fields surrounding the γ″ precipitates. New, higher performance alloys reinforced by γ″ precipitates must therefore focus on increasing the stability of the γ″ against the transformation to the δ phase, whilst also restricting the coarsening behaviour of the γ″ to maintain optimal mechanical properties. To this end, the increased volume fraction of γ′ in this alloy aids the stability of the γ″ phase by impeding the passage of the dislocations that are necessary for the formation of stacking faults within the γ″, which have been shown to be the pre-cursor for δ formation in IN718 and IN625 [6]. Furthermore, the increased volume fraction of γ′ precipitates also enhance the mechanical properties by requiring more complex dislocation structures to plastically deform the material [31,32].

To investigate the origins of the excellent tensile properties of this alloy, HAADF STEM images were obtained from a sample subjected to tensile testing at 700 °C. The images acquired, Fig. 4b, showed significant strain in the γ matrix induced by the presence of the precipitates and evidence of the γ′ and γ″ precipitates having been sheared by the passage of dislocations. Imaging at higher magnification, Fig. 4c, showed that the γ′ precipitates were cleanly sheared, resulting in a lateral displacement above and below the slip plane (red arrow), whereas, the γ″ precipitates exhibited smaller displacements within each precipitate (blue arrow). Whilst the specific dislocation structures and deformation mechanisms are yet to be fully characterised, the differing interactions of the dislocations with the γ′ and γ″ precipitates, as well as the high strain in the matrix, are hypothesised to provide considerable resistance to dislocation motion, thereby leading to the high tensile strength of this alloy. The excellent strength of the dual-superlattice superalloy is even

more remarkable given its relative compositional simplicity and given the data presented in Fig. 3, it is clear that further improvements could be obtained through higher order alloying. However, whilst the initial results are promising, it is recognised that these alloys will need to demonstrate a balance of properties, including adequate creep, fatigue, oxidation, corrosion and dwell fatigue resistance if they are to find use in gas turbine engines.

Acknowledgments

The authors are grateful to Profs. D. Rugg, W.J. Clegg and N.D. Mathur for their comments, and acknowledge the EPSRC/Rolls-Royce Strategic Partnership for funding (EP/M005607/1 and EP/H022309/1) and the Diamond Light Source for provision of beam time (EE9270).

References

[1] J.H. Perepezko, Science 326 (2009) 1068–1069.
[2] C.T. Sims, N.S. Stoloff, W.C. Hagel (Eds.), Superalloys II, Wiley-Interscience, New York, 1987.
[3] M. Durand-Charre, The Microstructure of Superalloys, Gordon and Breach, Amsterdam, 1997.
[4] D.F. Paulonis, J.M. Oblak, D.S. Duvall, ASM Trans. Q. 62 (1969) 611–622.
[5] J.M. Oblak, D.S. Duvall, D.F. Paulonis, Mater. Sci. Eng. 13 (1974) 51–56.
[6] M. Sundararaman, P. Mukhopadhyay, S. Banerjee, Metall. Trans. A. 19 (1988) 453–465.
[7] C. Slama, M. Abdellaoui, J. Alloys Compd. 306 (2004) 277–284.
[8] R. Cozar, A. Pineau, Metall. Trans. A. 4 (1973) 47–59.
[9] J.P. Collier, S.H. Wong, J.C. Phillips, J.K. Tien, Metall. Trans. A. 19 (1988) 1657–1666.
[10] P.M. Mignanelli, N.G. Jones, M.C. Hardy, H.J. Stone, Mater. Sci. Eng. A 612 (2014) 179–186.
[11] P.M. Mignanelli, H.J. Stone, N.G. Jones, M.C. Hardy, UK Patent Application Number GB1512692.3, 2015.
[12] L. Viskari, K. Stiller, Ultramicroscopy 111 (2011) 652–658.
[13] A. Oradei-Basile, J.F. Radavich, Superalloys 718, 625 and Various Derivatives, 1991 625-335.
[14] J.A. Manriquez, P.L. Bretz, L. Rabenburg, J.K. Tien, Superalloys 1992 (1992) 507–516.
[15] D.P. Mourer, K.R. Bain, United States Patent 8,613,810, 2013.
[16] K.R. Bain, et al., United States Patent 8,992,699, 2015.
[17] M.C. Hardy, United States Patent 9,074,476, 2015.
[18] M. Gao, D.J. Dwyer, R.P. Wei, Scr. Mater. 32 (1995) 1169–1174.
[19] Allegheny Technologies Incorporated, ATI 718Plus Alloy, https://www.atimetals.com/Documents/ati_718plus_tds_en_v3.pdf 2013.
[20] Haynes International, "Pocket Guide to High Temperature Properties of Age-hardenable High Performance Alloys" (H-3127B), 2002.
[21] Haynes International, "Heaynes 282 Alloy" (H-3173A), 2008.
[22] Special Metals Corporation, "Inconel Alloy 718" (SMC-045), 2007.
[23] Special Metals Corporation, "Incoloy Alloy 909" (SMC-077), 2004.
[24] T.P. Gabb, J. Telesman, P.T. Kantzos, J. Fail. Anal. Prev. 7 (2007) 56–65.
[25] J.-Y. Guedou, I. Augustines-Lecallier, L. Naze, P. Caron, D. Locq, Superalloys 2008 (2008) 21–30.
[26] J.F. Barker, E.H. VanDerMolen, Superalloys 1972 (1972) AA1–AA23.
[27] R.J. Mitchell, Development of a New Powder Processed Ni-base Superalloy for Rotor Disc Applications, University of Cambridge, 2004.
[28] J.H. Moll, J.J. Conway, Superalloys 2000 (2000) 135–142.
[29] K.-M. Chang, United States Patent 4,981,644, 1991.
[30] K.R. Ziegler, J.F. Wallace, Superalloy 718 (1989) (1989) 611–622.
[31] D. McAllister, D. Lv, B. Peterson, H. Deutchman, Y. Wang, M.J. Mills, Scr. Mater. 115 (2016) 108–112.
[32] D.C. Lv, D. McAllister, M.J. Mills, Y. Wang, Acta Mater. 118 (2016) 350–361.